Supporting Information

Local electronic structure of the peptide bond probed by resonant inelastic soft x-ray scattering

L. Weinhardt[1,2,3,*], A. Benkert[1,4], F. Meyer[4], M. Blum[3,5], D. Hauschild[1,2], R.G. Wilks[6], M. Bär[6,7,8], W. Yang[5], M. Zharnikov[9], F. Reinert[4], and C. Heske[1,2,3]

[1]*Institute for Photon Science and Synchrotron Radiation (IPS), Karlsruhe Institute of Technology (KIT), Hermann-v.-Helmholtz-Platz 1, 76344 Eggenstein-Leopoldshafen, Germany*

[2]*Institute for Chemical Technology and Polymer Chemistry (ITCP), Karlsruhe Institute of Technology (KIT), Engesserstr. 18/20, 76128 Karlsruhe, Germany*

[3]*Department of Chemistry and Biochemistry, University of Nevada, Las Vegas (UNLV), 4505 Maryland Parkway, NV 89154-4003, USA*

[4]*Universität Würzburg, Experimentelle Physik VII, Am Hubland, 97074 Würzburg, Germany*

[5]*Advanced Light Source (ALS), Lawrence Berkeley National Laboratory, 1 Cyclotron Road, Berkeley, CA 94720, USA*

[6]*Interface Design, Helmholtz-Zentrum Berlin für Materialien und Energie GmbH, Albert-Einstein-Str. 15, 12489 Berlin, Germany*

[7]*Helmholtz-Institute Erlangen-Nürnberg for Renewable Energy, Forschungszentrum Jülich, Egerlandstr. 3, 91058 Erlangen, Germany*

[8]*Physical Chemistry II, Department of Chemistry and Pharmacy, Friedrich-Alexander-Universität Erlangen-Nürnberg, Egerlandstr. 3, 91058 Erlangen, Germany*

[9]*Angewandte Physikalische Chemie, Universität Heidelberg, Im Neuenheimer Feld 253, 69120 Heidelberg, Germany*

*corresponding author: lothar.weinhardt@kit.edu

Radiation damage study:

Organic compounds are generally very sensitive to x-ray irradiation, exhibiting radiation damage already after short exposure times. This can strongly influence the measured x-ray emission (XES) and absorption (XAS) spectra. To characterize and minimize the spectral radiation impact in this study, we have measure a series of XES spectra with varying exposure times (by scanning the sample) and reduced beamline flux (by detuning the undulator). Figure S1 shows the spectra collected for diglycine (left) and triglycine (right). The spectral shape shows strong variations as a function of dose, but remains unchanged for the lowest exposures (with significantly reduced flux). For both compounds, no further spectral changes are observed between the two lowest doses (0.09 s at 15% flux and 0.07 s at 8% flux). Consequently, we have chosen 0.09 s per point at 15% flux for the XES and XAS measurements presented in this paper, such that radiation damage effects in the spectra can be neglected.
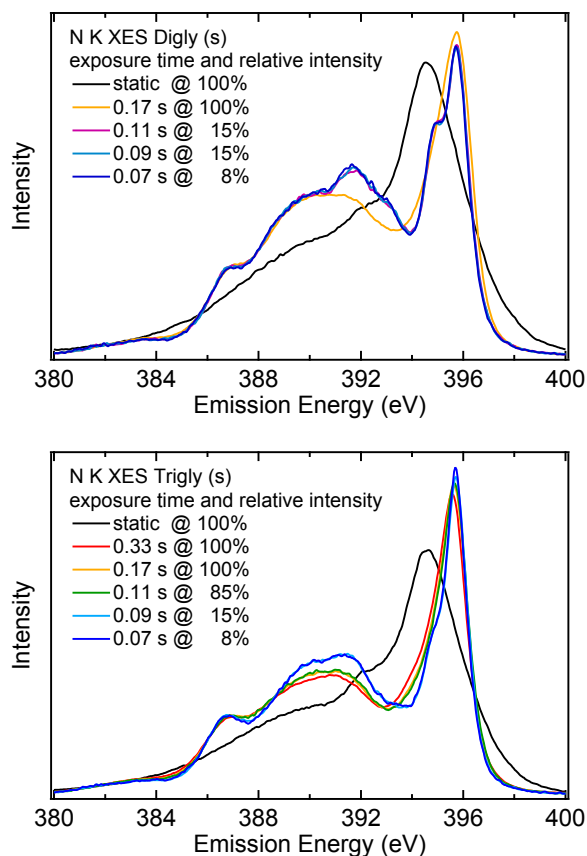
Figure S1: N K XES spectra of solid-state diglycine (left) and triglycine (right), recorded with the given values for exposure time of each sample spot and excitation intensities. The black spectra represent the static measurement, i.e., a completely decomposed sample, whereas the dark blue spectra were recorded with the lowest-dose parameters.

Spectra calculations:

XES and XAS spectra of isolated zwitterionic glycine, diglycine, and triglycine molecules were calculated using density-functional theory (DFT) within the StoBe-DeMon package[1]. Becke and Perdew exchange and correlation functionals[2–4] were used for geometry optimization and single-point calculations. For the hydrogen and carbon atoms, the valence electrons were described by a double-zeta basis[5] and effective core potentials (ECPs)[6] with a 321/311/1 basis set, respectively. In the case of the nitrogen and oxygen atoms, a triple-zeta basis[5] was used. Core-excited atoms were described using diffuse IGLO-III basis sets[7]. The XES transition probabilities were calculated based on the ground-state Kohn–Sham eigenstates, while, for the XAS transition probabilities, the half core-hole transition potential method was used. The transitions energies were calculated with a Δ(Kohn–Sham self-consistent field) approach that includes differential relativistic effects associated with the removal of one electron from the 1s orbital[8]. Only small additional shifts were necessary to align the calculated emission energies with the experimental spectra and are given in Table S1.

Table S2 lists prominent spectral features and their tentative assignment to transitions from the different valence orbitals.

Figures S1, S2, and S3 show the molecular structure and calculated iso-density surfaces of the occupied molecular orbitals of glycine, diglycine, and triglycine, respectively.

Table S1: Energy shifts (in eV) used to align the calculated spectra with the experimental data.

	XES		XAS	
	N K	O K	N K	O K
Glycine		+0.4	−1.4	−1.2
Diglycine	+0.7	+0.8	−1.1	−1.6
Triglycine	0	+0.6	−1.2	−1.2

Table S2: Emission energies of prominent spectral features (in eV) and tentative assignment to valence orbitals and, in parentheses, to sites involved in the corresponding transitions.

|	N K		O K	
	Energy (eV)	Valence Orbital(s)	Energy (eV)	Valence Orbital(s)
Glycine	397.0	HOMO – HOMO-5	526.8	HOMO, HOMO-1/2 (O1, O2)
	394.9	Dissociation "–NH$_2$"	522.5	HOMO-3/4/5 (O1,O2)
	386 – 394	HOMO-8/9/10/11		
Diglycine	395.8	HOMO-3 (N2)	526.8	HOMO, HOMO-1/2 (O1, O2), HOMO-3/4 (O3)
	394.9	Dissociation "–NH$_2$"		
	391.9	HOMO-10/11/12 (N2)	524.9	HOMO-8 (O3)
	386.8	HOMO-15 (N2)	523.9	HOMO-9 (O3)
			522.5	HOMO-5/6/7 (O1,O2)
Triglycine	395.8	HOMO-3 (N2), HOMO-7 (N3)	526.8	HOMO, HOMO-1/2 (O1, O2), HOMO-3/4 (O3), HOMO-7/8 (O4)
	394.9	Dissociation "–NH$_2$"		
	391.6	HOMO-14 (N2)	524.9	HOMO-10/11 (O3)
	389.8	HOMO-19 (N3)	523.9	HOMO-15/16 (O4)
	386.8	HOMO-21 (N2), HOMO-24 (N3)	522.5	HOMO-5/6/8 (O1,O2)
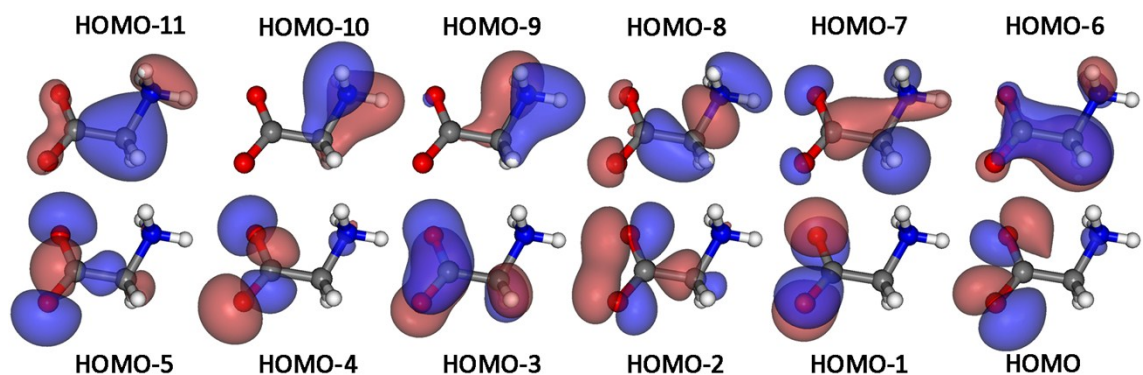
Figure S2: Molecular structure and calculated orbital iso-density surfaces of the occupied molecular orbitals of glycine.
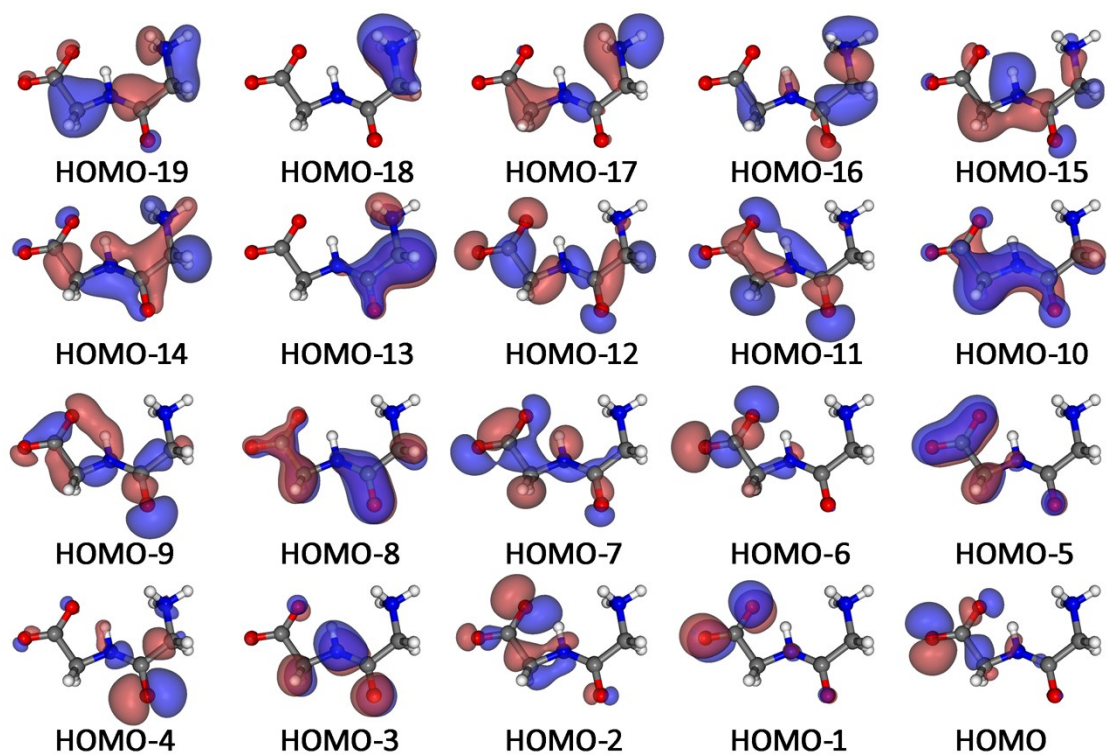

Figure S3: Molecular structure and calculated orbital iso-density surfaces of the occupied molecular orbitals of diglycine.

HOMO-27   HOMO-26   HOMO-25   HOMO-24

HOMO-23   HOMO-22   HOMO-21   HOMO-20

HOMO-19   HOMO-18   HOMO-17   HOMO-16

HOMO-15   HOMO-14   HOMO-13   HOMO-12

HOMO-11   HOMO-10   HOMO-9   HOMO-8

HOMO-7   HOMO-6   HOMO-5   HOMO-4
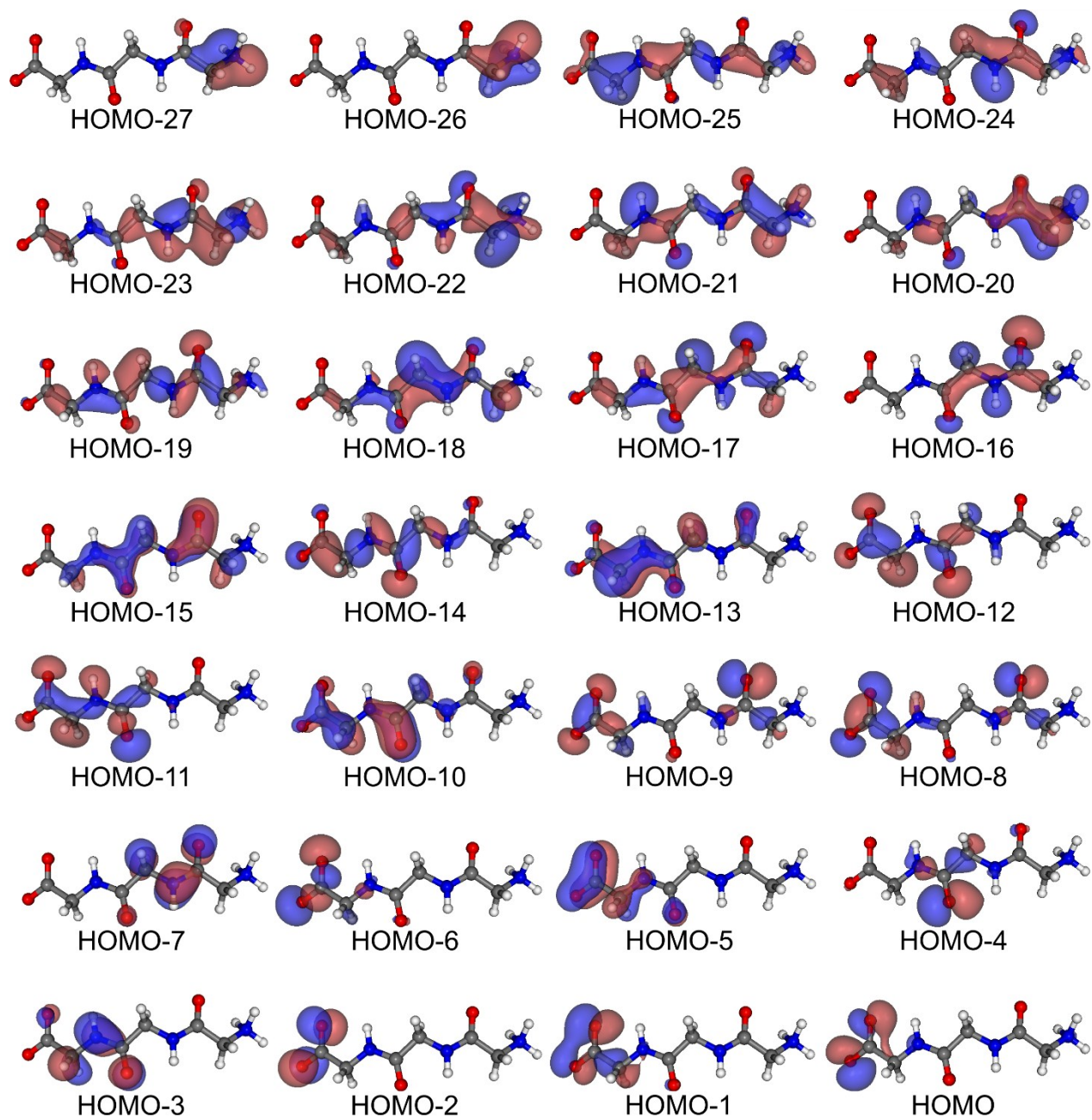
HOMO-3   HOMO-2   HOMO-1   HOMO

Figure S4: Molecular structure and calculated orbital iso-density surfaces of the occupied molecular orbitals of triglycine.

1 K. Hermann, L. G. M. Pettersson, M. E. Casida, C. Daul, A. Goursot, A. Koester, E. Proynov, A. St-Amant and D. R. Salahub, Contributing Authors: V. Carravetta, H. Duarte, C. Friedrich, N. Godbout, J. Guan, C. Jamorski, M. Leboeuf, M. Leetmaa, M. Nyberg, S. Patchkovskii, L. Pedocchi, F. Sim, L. Triguero, and A. Vela, StoBe-DeMon Version 3.1 (2011).

2 A. D. Becke, *Phys. Rev. A*, 1988, **38**, 3098–3100.

3 J. P. Perdew, *Phys. Rev. B*, 1986, **33**, 8822–8824.

4 J. P. Perdew, *Phys. Rev. B*, 1986, **34**, 7406–7406.

5 N. Godbout, D. R. Salahub, J. Andzelm and E. Wimmer, *Can. J. Chem.*, 1992, **70**, 560–571.

6 L. G. M. Pettersson, U. Wahlgren and O. Gropen, *J. Chem. Phys.*, 1987, **86**, 2176–2184.

7 W. Kutzelnigg, U. Fleischer and M. Schindler, *The IGLO-Method: Ab-initio Calculation and Interpretation of NMR Chemical Shifts and Magnetic Susceptibilities". in "Deuterium and Shift Calculation. NMR Basic Principles and Progress"*, Springer, Heidelberg, 1990.

8 L. Triguero, L. G. M. Pettersson and H. Ågren, *Phys. Rev. B*, 1998, **58**, 8097–8110.